International Journal of Medical, Medicine and Health Sciences
ISSN: 2517-9969
Vol:6, No:4, 2012

Automatic Detection of Mass Type Breast Cancer using Texture Analysis in Korean Digital Mammography

E. B. Jo, J. H. Lee, J. Y. Park and S. M. Kim

***Abstract*—**In this study, we present an advanced detection technique for mass type breast cancer based on texture information of organs. The proposed method detects the cancer areas in three stages. In the first stage, the midpoints of mass area are determined based on AHE (Adaptive Histogram Equalization). In the second stage, we set the threshold coefficient of homogeneity by using MLE (Maximum Likelihood Estimation) to compute the uniformity of texture. Finally, mass type cancer tissues are extracted from the original image. As a result, it was observed that the proposed method shows an improved detection performance on dense breast tissues of Korean women compared with the existing methods. It is expected that the proposed method may provide additional diagnostic information for detection of mass-type breast cancer.

***Keywords*—**Mass Type Breast Cancer, Mammography, Maximum Likelihood Estimation (MLE), Ranklets, SVM

I. Introduction

THE detection of the breast cancer from mammographic images is one of the fundamental challenges in medical image applications [1]-[3]. Despite these applicabilities, the accuracy for detecting mass-type breast cancer is still remained as 80% [4]-[6]. In particular, dense breast shows the low penetrability due to the dense composition of the breast tissues, and thereby presenting the low accuracy for the cancer detection [7], [8]. Asian women including Korean women typically have denser breasts than other women. The existing detection methods, therefore, present the relatively low accuracy for the mass type breast cancer in Asian women.

To solve these limitations, Karseemeijer et al., suggested a diagnostic method which uses the degree of texture on tissues in the relevant area heading toward center after obtaining gradients of pixels in the cancer area [4]. Brake et al., improved detection performance on mass type breast cancer by applying Karseemeijer's algorithm in a multi-scale method [9]. Huang et al., converted shape and type of mass into one dimensional profile by combining gradient and binary information, and suggested peak and bottom based detection method [10]. On the other hand, Mudigonda et al., detected an area of major directivity by calculating correlation between gradients and pixel values belonged to a fixed-size window [11].

E. B. Jo is with the Department of Medical Bio Technology, Dongguk University, Seoul, Korea. (e-mail: eunbyeol27@gmail.com).
J. H. Lee is with the Department of Medical Bio Technology, Dongguk University, Seoul, Korea. (e-mail: tupac1969@gmail.com)
J. Y. Park is with the Department of Medical Bio Technology, Dongguk University, Seoul, Korea. (e-mail: pipen@nate.com)
S. M. Kim is with the Department of Medical Bio Technology, Dongguk University, Seoul, Korea. (e-mail: smkim@dongguk.edu)

However, current diagnostic techniques still have several limitations in spite of these numerous efforts. Firstly, the existing methods show technical difficulties to determine the directivity of the pixel gradient due to the slight variation of the original image. Secondly, the detection accuracy of the cancer is relatively low in dense breast tissues.

In this study, we present an advanced detection technique for mass type breast cancer based on texture information of organs to solve these limitations. The proposed method detects the cancer areas in three stages. In the first stage, the midpoints of mass area are determined based on AHE (Adaptive Histogram Equalization). In the second stage, we set the threshold coefficient of homogeneity by using MLE (Maximum Likelihood Estimation) to compute the uniformity of texture. Finally, mass type cancer tissues are extracted from the original image. The rest of the paper is organized as follows: Section 2 introduces the details of the proposed algorithm. Section 3 gives the experimental results of the proposed method. Finally, we conclude our findings in section 4.

II. Materials and Methods

A. Detection of Midpoint in a Mass Area

AHE can clearly differentiate ROI (Region of Interest) from background in images by adaptively increasing contrast of images [12]. In other words, it is possible to determine a single threshold which can select ROI on all mass areas using AHE [13], [14]. Through repetitive applications of this concept on the original images, peripheral points can be removed, and only the area including midpoint of masses remains. The final midpoint position of each mass is derived from the center of the gravity of each detected area. Fig. 1 shows the removal procedure of the neighborhood peak points.

The process obtaining a midpoint of mass area from original images is as follows:

Step 1: We designated $I^0(i, j)$ as brightness of pixel at an image coordinate (i, j).

Step 2: AHE is applied to image I^k where k = 0, 1, 2, …, L.

Step 3: Non- interest areas are removed from the $I^k(i, j)$, and updated it to $I^{k+1}(i, j)$ as following equation (1).

$$I^{k+1}(i,j) = \begin{cases} I^k(i,j) & for \quad I^k(i,j) \geq T_c \\ 0 & for \quad I^k(i,j) < T_c \end{cases} \qquad (1)$$

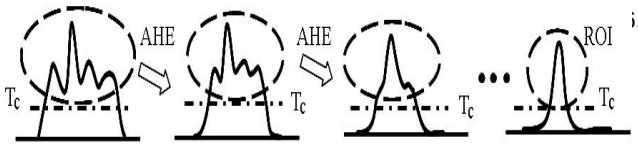

* AHE : Adaptive Histogram Equalization

Fig. 1 The removal procedure of the neighborhood peak points

Threshold T_c is designated at 50% of maximum brightness of images as shown in equation (2).

$$T_c = 0.5 \times \max\left\{I^k(i,j)\right\} \tag{2}$$

Step 4: Step 1 and step 2 are conducted L times (L=10).

Step 5: Detected areas are designated as ROI. In other words, if N detected areas are present, ROI_s satisfy ROI_1, ROI_2, …, and ROI_N. In case that designated number of pixel of ROI is less than 25, we assumed the detected area as image noise, and excluded from the calculation process.

Step 6: Center of gravity of each ROI is determined, and it is designated as a midpoint of mass. Midpoint (C^n_i, C^n_j) of mass corresponding to n^{th} ROI can be computed by equation (3).

$$C_i^n = \frac{\sum_{i \in ROI} i \cdot I(i,j)}{\sum_{i \in ROI} I(i,j)}, \quad C_j^n = \frac{\sum_{j \in ROI} j \cdot I(i,j)}{\sum_{j \in ROI} I(i,j)} \tag{3}$$

Fig. 2 demonstrates the entire extraction process of the peak point for the dense breast image by using AHE method.

B. Determination of Radius of Mass Area

In general, the mass area is brighter than the background area in the dense breast image [15]. Brightness value reduces as the radius from the midpoint of mass increases, and the value converges to a constant level when the radius breaks away from the mass area. By contrast, the brightness value increases again as a mass area appears nearby. Based on this concept, we considered that the radius belongs to the surrounding mass area, when brightness value reveals three consecutive times within a certain range. We determined that the radius breaks away from the mass area in the opposite case.

The mean pixel value at radius r from the center of mass can be calculated as equation (4).

$$C(r) = \frac{1}{N_r} \sum_{(i,j) \in C_r} I(i,j), \quad r = 1,2,\cdots \tag{4}$$

I(i, j) indicates brightness value of images, and r is a radius from the center of mass, r = |i| +|j|. C_r means a coordinate of a pixel on radius r satisfying $C_r = \{(i, j) \mid |i| + |j| = r\}$, and N_r is a number of pixels on radius r satisfying $N_r = |C_r| = 4r$. Radius of mass area is computed by equation (5).

$$r_{mass} = \min\left\{r^1, r^2\right\} \tag{5}$$

r^1, r^2 indicate each radius of mass area, respectively, and can be derived by equation (6) and (7)

$$r^1 = \arg\min_r \left\{ r \left| \frac{C(r-i-1) - C(r-i)}{C(r-i-1)} < \varepsilon \quad for\ i = 0,1,2 \right. \right\} \tag{6}$$

$$r^2 = \arg\min_r \left\{ r \left| C(r-i) - C(r-i-1) > 0 \quad for\ i = 0,1,2 \right. \right\} \tag{7}$$

where the threshold value on the C(r) is 0.1.

C. Detection of Homogeneous Mass Tissues using Homogeneity

Mass-type breast cancer usually spreads from the center section to the peripheral tissues. Accordingly, uniform texture is revealed at the center section, and the peripheral tissue presents the non-uniform texture [16], [17]. The area that contains uniform texture at the center section is therefore likely to be the cancer tissues. In order to measure uniformity of texture, we computed homogeneity (H) from the original image by equation (8).

$$H = \sum_{i \le M} \sum_{j \le M} \frac{P(i,j)}{1 + |i-j|} \tag{8}$$

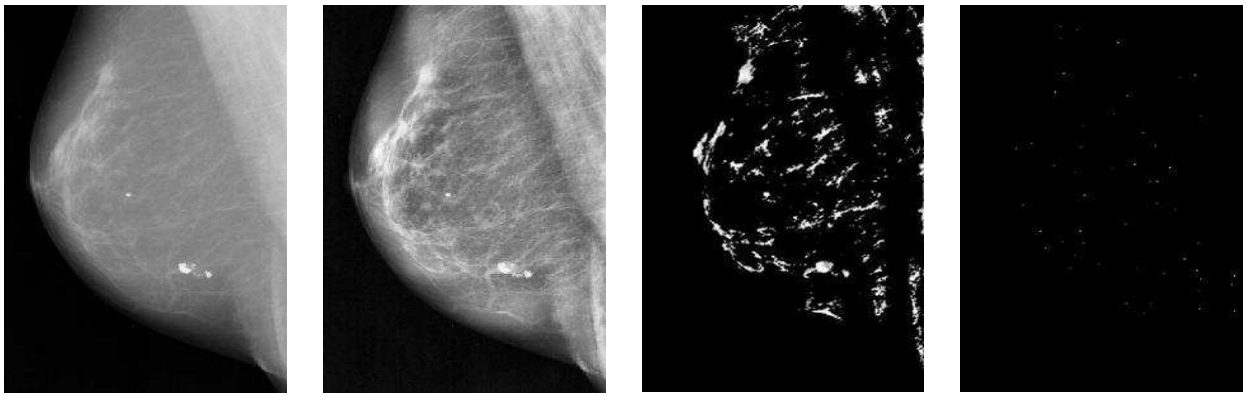

(a) Original Image (b) AHE image (1 time) (c) AHE image (18 times) (d) Centers of masses

Fig. 2 Extraction process of the peak point for the dense breast image based on AHE method

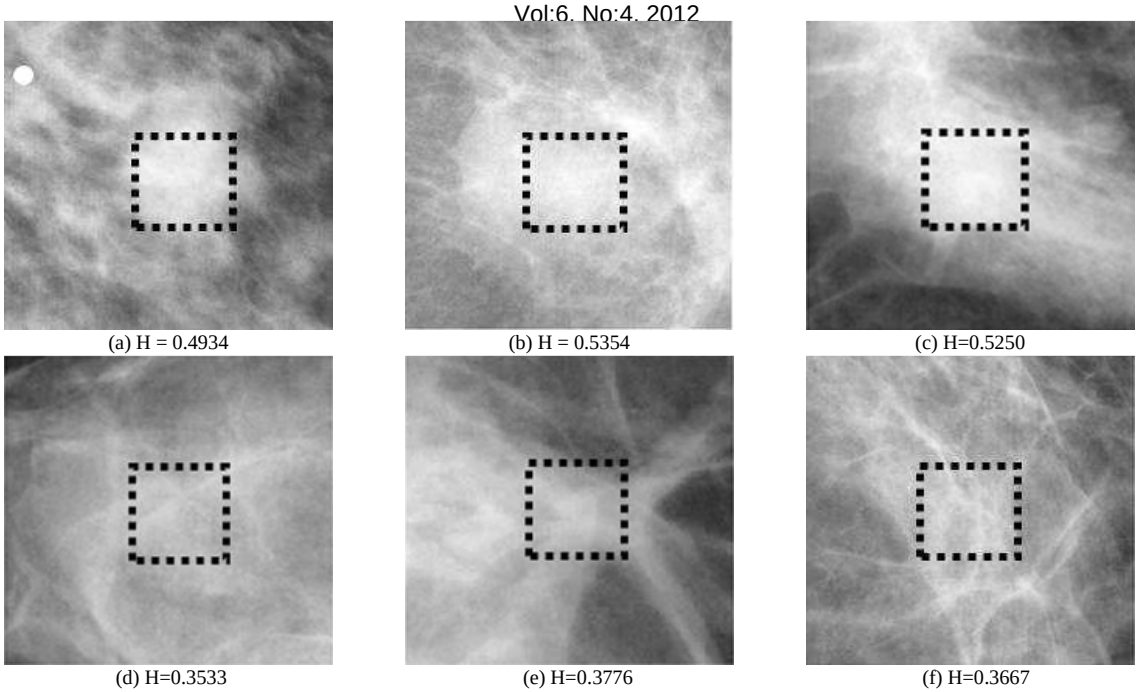

(a) H = 0.4934 (b) H = 0.5354 (c) H=0.5250

(d) H=0.3533 (e) H=0.3776 (f) H=0.3667

Fig. 3 Preliminary results on differentiating normal tissues from cancer tissues using homogeneity

In the equation (8), P(i,j) indicates a co-occurrence matrix with a vertical and horizontal distance of 1, respectively, and M represents size of the center section of the mass area. M is adjusted at 20% of the total size of the mass area, and size of the co-occurrence matrix was set to 5x5. In addition, we applied threshold to the homogeneity by employing maximum likelihood estimation (MLE) method to extract the mass area more precisely. Fig. 3 represents results of the preliminary experiments on differentiating normal tissues from cancer tissues based on homogeneity. In the case of cancer tissues, homogeneity revealed large mainly due to the homogeneous center section of mass area. On the other hand, normal tissues presented a small homogeneity. As a result, it was observed that the homogeneity could differentiate the cancer tissues from the normal in a dense breast image.

Fig. 4 presents the distribution of the homogeneity coefficients derived from 182 cancer and 996 normal tissues. Based on this distribution, the optimal threshold for homogeneity is revealed as 0.4. When threshold of 0.4 was employed, however, the detection accuracy was low as missing rate reached over 10%. We therefore selected the threshold value as 0.37 to minimize the missing rate, and thereby set the missing rate lower than 5%. Fig. 5 shows vertical, horizontal and diagonal areas to measure relative brightness of the mass area.

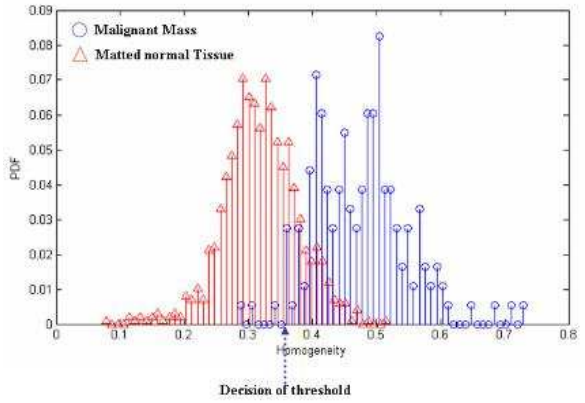

Fig. 4 Distribution of the homogeneity coefficients between 182 cancer and 996 normal tissues

D.Measurement of Directivity of Texture using Ranklets

Directivity of texture on the area including center of mass at horizontal, vertical and diagonal directions can be derived by using Ranklets method as shown in fig. 5 [18], [19]. In order to detect mass-type breast cancer in the image, we determined whether directivity of texture is heading for the center of mass [20]. Coefficient of comparative brightness grade W^i_{YX} tends to increase in number of bright pixels more in T_i area than in area $C_i$at the same position. Coefficient of comparative brightness grade W^i_{YX} can be computed by equation (9)

$$W^i_{YX} = x \in T_i \left\{ \pi(x) - \frac{N(N+1)}{2} \right\} \quad (9)$$

where x indicates values of pixels belonging to T_i, and N is number of total pixels. Rank transformation π converts pixel values to relative grades. The Ranklets coefficients corresponding to vertical, horizontal and diagonal lines can be derived by equation (10) [20].

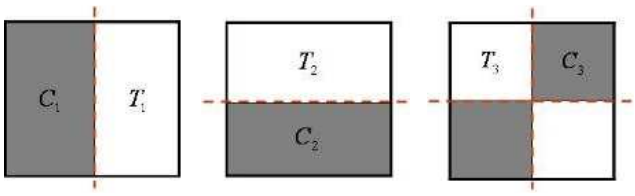

(a) Vertical (b) Horizontal (c) Diagonal

Fig. 5 Directional areas for measuring relative brightness

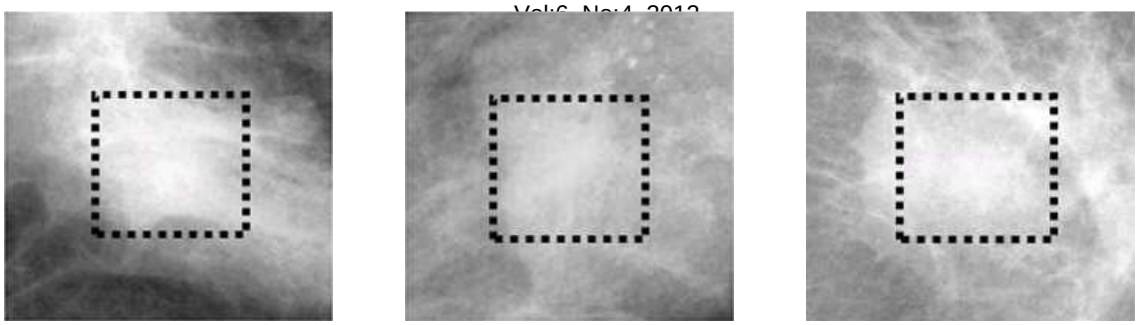

(a) Three cancer tissues

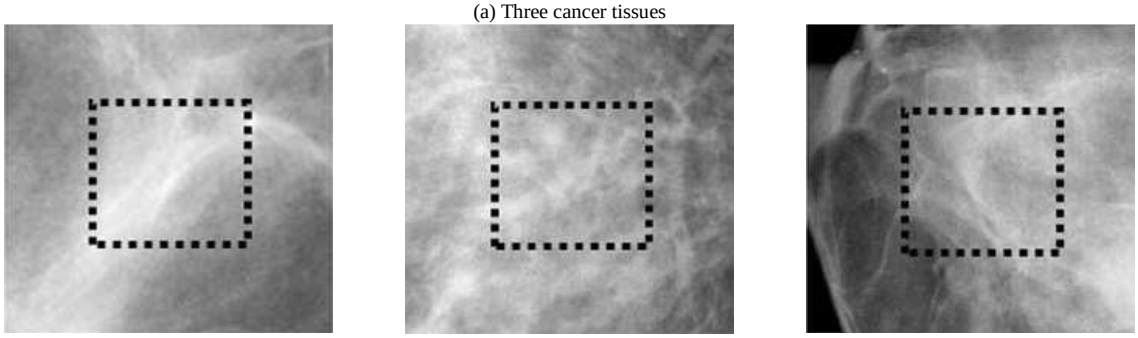

(b) Three normal tissues

Fig. 6 Mass area composed of three cancer tissues (above) and three normal tissues (below)

$$R_i = \frac{2W_{YX}^i}{N^2/4} - 1, \quad i = v, h, d \tag{10}$$

Ranklets were calculated at only 40% of the total mass area. In addition, texture analysis is inefficient in the case of the 100 um/pixel resolutions, since changes in neighboring pixels hardly occur. Resolution of the original images was therefore down-sampled at 400 um/pixel. As a consequence, we observed clear texture form as differences among pixels were distinctly shown, and computational load was also decreased.

TABLE I
DIRECTIVITY OF NORMAL AND CANCER AREAS

	(a)	(b)	(c)	(d)	(e)	(f)
V	0.17	-0.12	0.04	-0.51	-0.61	0.66
H	0.25	0.20	-0.25	0.07	0.22	0.14
D	0.26	-0.35	0.18	-0.66	-0.18	0.12

V: Vertical, H: Horizontal, D: Diagonal

III. Experimental Results

In this study, Ranklets model was formed through SVM using Ranklets vectors measured in the center section of drawn area to detect mass-type breast cancer. Fig. 6 presents a mass area including 3 cancer tissues (above), and a mass area including 3 normal tissues (below). The center section area for measuring Ranklets was indicated with a dotted line, and the size of the window was designated at 40% of the total mass area. Table 1 represents vertical, horizontal and diagonal Ranklets of each mass image. Through these Ranklets, we assessed directivity of texture. The texture directivity increases as the Ranklets value increases, where the texture directivity decreases, when the Ranklets value decreases. We thus determined that no directivity indicates the neutralization of the Ranklets due to the same directivity for the center.

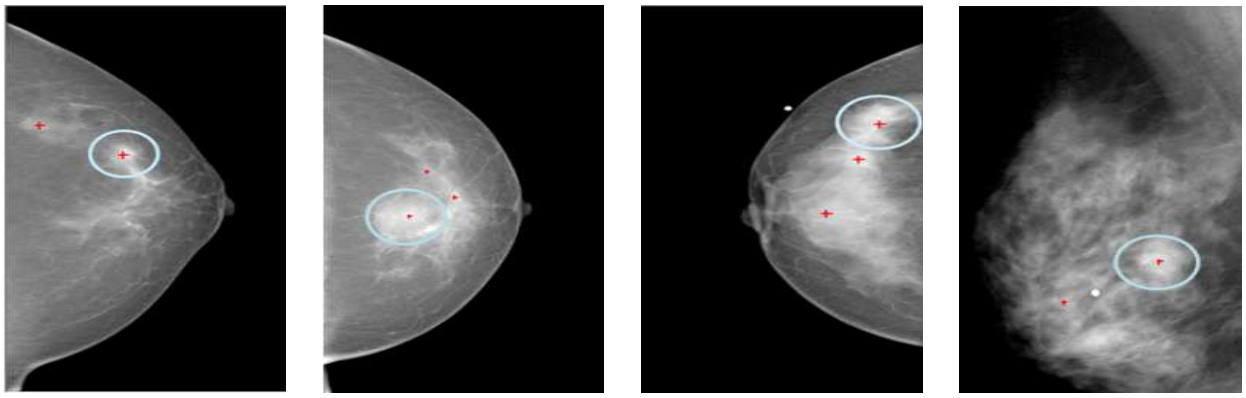

Fig. 7 Experimental result of the proposed method on the dense breast

The proposed detection method presented an 85.4% of true alarm rate at a total of 82 cases of mass-type breast cancer, and the number of false alarm per image was shown as 2.6. Fig. 7 shows the experimental results of the proposed method for dense breast images. The area with red dots indicates pre-diagnosed cancer area, while the circular area presents the newly detected area by the proposed method.

IV. Conclusion

In this study, we proposed an advanced detection technique for mass type breast cancer based on texture information of organs to solve these limitations. The proposed method detected the cancer areas in three stages. In the first stage, the midpoints of mass area were determined based on AHE. In the second stage, we set the threshold coefficient of homogeneity by using MLE to compute the uniformity of texture. Finally, mass type cancer tissues were extracted from the original image. As a result, it was observed that the proposed method shows an improved detection performance on dense breast tissues of Korean women compared with the existing methods.Since mass type breast cancer is found in the various and complicated forms, reviews and analyses on each feature of the cancer are required. It is thus expected that the development of image analysis methods applicable to the morphological features of cancer can contribute to develop an early detective system for breast cancer.

Acknowledgment

This work was supported by the Dongguk University Research Fund.

References

[1] L. Zhan, Y. Ren, C. Huang, F. Liu, "A novel automatic tumor detection for breast cancer ultrasound Images," *Eighth International Conference on Fuzzy Systems and Knowledge Discovery (FSKD)*, vol. 4, pp. 401-404, July. 2011.

[2] V. Nadvoretskiy, S. Ermilov, "Image processing and analysis in a dual-modality optoacousitc/ultrasonic system for breast cancer diagnosis" *2011 Society of Photo-Optical Instrumentation Engineers (SPIE)*, vol. 12, pp. 7899-08, Jan. 2011.

[3] B. Liu, H.D. Cheng, J. Huang, J. Tian, X. Tang, J. Liu, "Fully automatic and segmentation-robust classification of breast tumors based on local texture analysis of ultrasound images", *Pattern Recognit*. vol. 43, pp.280-298, Jan. 2010.

[4] N. Karssemeijer, "Detection of stellate distortions in Mammograms," *IEEE Trans. Med. Imaging*, vol. 15, pp. 611-619, Oct. 1996

[5] M. Kevin, W. Kelly, Judy Dean, L. Sung-Jaee, "Breast cancer detectio n using automated whole breast ultrasound and mammography in radi ographically dense breasts" *Eur. Radiol*, vol. 20, pp. 734-742, 2010.

[6] A. I. Phipps, C. I. Li, K. Kerlikowske, W. E. Barlow, "Risk factors for ductal, lobular, and mixed ductal-lobular breast cancer in a screening population." *Cancer Epidemiol. Biomarkers Prev.* vol. 19, pp. 1643-1654, May. 2010.

[7] K. Ghosh, K. R. Brandt, C. Reynolds, CG Scott, "Tissue composition of mammographically dense and non-dense breast tissue" *Breast Canc er Res. Treat*, vol. 131 pp. 267-275, 2012.

[8] J. Ding , R. Warren, A. Girling, D. Thompson, "Mammographic Densi ty, Estrogen Receptor Status and Other Breast Cancer Tumor Characte ristics". *Breast J*, vol. 16, pp. 279-289, Jun. 2010.

[9] M. Guido, T. Brake, N. Karssemeijer, "Single and multiscale detection of masses in digital mammograms", *IEEE Trans. Medical Imaging*, v ol. 18, no. 7, pp-628-639, July. 1999.

[10] H. Sheng Fang, C. Ruey Feng, C. Dar Ren, D. Chen, "Characterization of speculation on ultrasound lesions." *IEEE Trans. Medical Imaging*, vol. 18, no. 7, pp. 628-639, July. 1999.

[11] N. R. Mudigonda, R. M Rangayyan, J. E Leo Desautels, "Detection of Breast Masses in Mammograms by Density Slicing and Texture Flow-Field Analysis", *IEEE Trans.Med.Imag*, vol. 20, no. 12, pp. 1215-1227, Dec. 2001.

[12] Q. Zhi, Y. Zhuangzhi, W. Shengqian, "Mammographic Feature Enha ncement Based on Second generation Curvelet Transform" *2010 3rd In ternational Conference on Biomedical Engineering and Informatics(B MEI 2010)*, vol. 7, pp. 349-353, Oct. 2010

[13] F. Moayedi, Z. Azimifar, R. Boostani, "Contourlet-based mammography mass classification using the SVM family" *Comput. Biol. Med*, vol. 40, pp. 373-383, April. 2010.

[14] S. Rathore, M. A Liftikhar, M. Hussain, "Texture Analysis for Liver Segmentation and Classification: A Survey" *2011 9th Frontiers of Information Technology(FIT)*, vol. 9, pp. 121-126, 2011.

[15] S. Don, E. Choi, M.Dugki, "Breast Mass Segmentation in Digital Mammography Using Graph Cuts" *Communication in computer and information science*, vol. 206, pp. 88-96, 2011.

[16] H. D. Cheng, Juan Shan, Wen Ju, Yanhui Guo, Ling Zhang, "Automat ed breast cancer detection and classification using ultrasound images: A survey". *Pattern Recognit*, vol. 43, pp. 299-317, Jan. 2010.

[17] G. Karbani, J. N. Lim, J. Hewison, "Culture, Attitude and Knowledge about Breast Cancer and Preventive Measurers: a Qualitative Study of South Asian Breast Cancer Pationts in the UK" *Asian Pac J Cancer Prev*, vol. 12, pp. 1619-26, 2011.

[18] H. D. Cheng, Juan Shan, Wen Ju, Yanhui Guo, Ling Zhang, "Automat ed breast cancer detection and classification using ultrasound images: A survey". *Pattern Recognit*. vol. 43, pp. 299-317, Jan. 2010.

[19] M. Khalid, R. Yusof, "A Comparative Study of Feature Extraction Methods for Woo Texture Classification" *2010 Sixth International Conference on Signal-Image Technology and Internet Based System*, vol. 17, pp. 23-29, 2010.

[20] S. Chen, B. Mulgrew, and P. M. Grant, "A clustering technique for digital communications channel equalization using radial basis function networks," *IEEE Trans. Neural Networks*, vol. 4, pp. 570–578, July 1993.